

## Dissipative Reactions with Intermediate-Energy Beams: A Novel Approach to Populate Complex-Structure States in Rare Isotopes

A. Gade<sup>1,2</sup>, B. A. Brown<sup>1,2</sup>, D. Weisshaar<sup>1</sup>, D. Bazin<sup>1,2</sup>, K. W. Brown<sup>1,3</sup>, R. J. Charity<sup>4</sup>, P. Farris<sup>1,2</sup>,  
A. M. Hill<sup>1,2</sup>, J. Li<sup>1</sup>, B. Longfellow<sup>1,2,\*</sup>, D. Rhodes<sup>1,2,†</sup>, W. Reviol<sup>5</sup>, and J. A. Tostevin<sup>6</sup>

<sup>1</sup>Facility for Rare Isotope Beams, Michigan State University, East Lansing, Michigan 48824, USA


<sup>2</sup>Department of Physics and Astronomy, Michigan State University, East Lansing, Michigan 48824, USA

<sup>3</sup>Department of Chemistry, Michigan State University, East Lansing, Michigan 48824, USA

<sup>4</sup>Department of Chemistry, Washington University, St. Louis, Missouri 63130, USA

<sup>5</sup>Physics Division, Argonne National Laboratory, Argonne, Illinois 60439, USA

<sup>6</sup>Department of Physics, Faculty of Engineering and Physical Sciences, University of Surrey, Guildford, Surrey GU2 7XH, United Kingdom

 (Received 27 August 2022; revised 11 October 2022; accepted 18 November 2022; published 7 December 2022)

A novel pathway for the formation of multiparticle-multipole excited states in rare isotopes is reported from highly energy- and momentum-dissipative inelastic-scattering events measured in reactions of an intermediate-energy beam of  $^{38}\text{Ca}$  on a Be target. The negative-parity, complex-structure final states in  $^{38}\text{Ca}$  are observed following the in-beam  $\gamma$ -ray spectroscopy of events in the  $^9\text{Be}(^{38}\text{Ca}, ^{38}\text{Ca} + \gamma)X$  reaction in which the scattered projectile loses longitudinal momentum of order  $\Delta p_{\parallel} = 700$  MeV/c. The characteristics of the observed final states are discussed and found to be consistent with the formation of excited states involving the rearrangement of multiple nucleons in a single, highly energetic projectile-target collision. Unlike the far-less-dissipative, surface-grazing reactions usually exploited for the in-beam  $\gamma$ -ray spectroscopy of rare isotopes, these more energetic collisions appear to offer a practical pathway to nuclear-structure studies of more complex multiparticle configurations in rare isotopes—final states conventionally thought to be out of reach with high-luminosity fast-beam-induced reactions.

DOI: 10.1103/PhysRevLett.129.242501

Beyond the proof of existence of a rare isotope and the determination of its ground-state half-life, the energies of excited states are typically the first observables that become accessible in laboratory experiments. For excited bound states, depending on their lifetime, prompt or delayed  $\gamma$ -ray spectroscopy is frequently used to obtain precise excitation energies from the measured transition energies [1]. In short-lived rare isotopes, excited states can be populated efficiently in (direct) nuclear reactions [2] or  $\beta$  decay [3], for example, most often exploiting the unique selectivity inherent to each of these different population pathways. The selectivity of one- and two-nucleon transfer and knockout reactions, or inelastic scattering [2,4–8], often enhances the population of excited states at moderate spin associated with the single-particle or collective degree of freedom. Here, we report the novel, complementary in-beam  $\gamma$ -ray spectroscopy of higher-spin, negative-parity states in  $^{38}\text{Ca}$  observed to be populated in the  $^9\text{Be}(^{38}\text{Ca}, ^{38}\text{Ca} + \gamma)X$  inelastic scattering at high-momentum loss. From the peculiar final states observed, we argue that these complex-structure, projectile excited states are formed by the rearrangement of multiple nucleons in a single, highly energetic projectile-target collision, giving access to multiparticle configurations not expected to be in reach of high-luminosity fast-beam reactions.

The reaction channel analyzed here is populated in the same experiment as reported in Ref. [9] where the focus was on  $^{40}\text{Sc}$  produced in the  $pn$  pickup reaction onto the  $^{38}\text{Ca}$  projectile. Here, we briefly summarize the experimental scheme below and refer the reader to Refs. [9,10] for more details. The  $^{38}\text{Ca}$  rare-isotope beam was produced by fragmentation of a stable  $^{40}\text{Ca}$  beam accelerated to 140 MeV/nucleon by the Coupled Cyclotron Facility at NSCL [11]. The momentum width transported to the experiment was restricted to  $\Delta p/p = 0.25\%$ , resulting in 160 000  $^{38}\text{Ca}/\text{s}$  impinging upon a 188-mg/cm<sup>2</sup>-thick  $^9\text{Be}$  foil located at the target position of the S800 spectrograph [12]. The setting subject of this publication ran for less than 40 hours. The constituents of the incoming beam and the projectilelike reaction products were identified on an event-by-event basis using the S800 analysis beam line and focal plane with the standard detector systems [13]. As the magnetic rigidity of the S800 spectrograph was tuned for  $^{36}\text{Ca}$ , only part of the outermost (exponential) low-momentum tail of the reacted  $^{38}\text{Ca}$  distribution was transmitted to the focal plane. Specifically, the S800 momentum acceptance at this setting is  $p_0 \pm 330$  MeV/c, with  $p_0 = 11.222$  GeV/c.

When compared to the parallel momentum distribution of the unreacted  $^{38}\text{Ca}$  passing through the target,

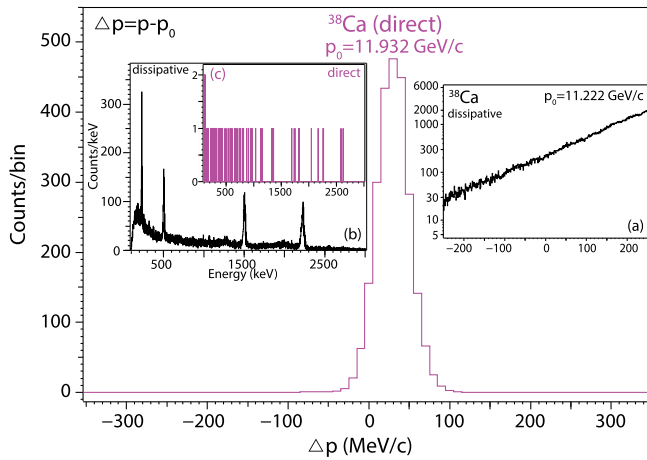


FIG. 1. Longitudinal momentum distributions of  $^{38}\text{Ca}$  passing through the target and only suffering energy loss (magenta peak) and, on log scale, for the dissipative setting [inset (a)]. Insets (b) and (c) confront the  $\gamma$ -ray spectra in coincidence with less than 100 500  $^{38}\text{Ca}$  at high-momentum loss (black) and from nearly 179 000  $^{38}\text{Ca}$  in the direct setting (magenta), highlighting a stark difference in excitation probability.

having suffered only in-target energy losses ( $p_0 = 11.932$  GeV/c), the low-momentum, reacted  $^{38}\text{Ca}$  events detected in the reaction setting have undergone an additional longitudinal momentum loss of about 700 MeV/c (see Fig. 1). That is, approximately 18 MeV/c per nucleon in momentum or 5.4 MeV/nucleon in energy. The cross section for finding  $^{38}\text{Ca}$  with such a large momentum loss was extracted to be  $\sigma(p_0 \pm 330 \text{ MeV/c}) = 3.8(4)$  mb, making these inelastic large-momentum-loss events rather rare.

The midtarget energy of  $^{38}\text{Ca}$  in the  $^9\text{Be}$  reaction target was 60.9 MeV/nucleon. The target was surrounded by GREINA [14,15], an array of 48 36-fold segmented high-purity germanium crystals assembled into modules of four crystals each, used for prompt  $\gamma$ -ray detection to tag the final states of the reaction residues. Signal decomposition was employed to provide the  $\gamma$ -ray interaction points. Of these, the location of the interaction with the largest energy deposition was selected as the first hit entering the event-by-event Doppler reconstruction of the  $\gamma$  rays emitted from the reaction residues in flight at about 33% of the speed of light [15].

The event-by-event Doppler reconstructed  $\gamma$ -ray spectrum obtained in coincidence with the  $^{38}\text{Ca}$  reaction residues detected in the S800 focal plane at large momentum loss is shown in Fig. 2. Nearest-neighbor adback, as detailed in Ref. [15], was used. Of the seven  $\gamma$ -ray transitions compiled in Ref. [16], those at 2213(5), 1489(5), 489(4), and 3684(8) keV are observed here, while the transitions at 214(4), 1048(6), 2417(7), 2537(6), 2688(7), and 2758(7) keV are reported for the first time in the present Letter. This Letter discusses the strongly

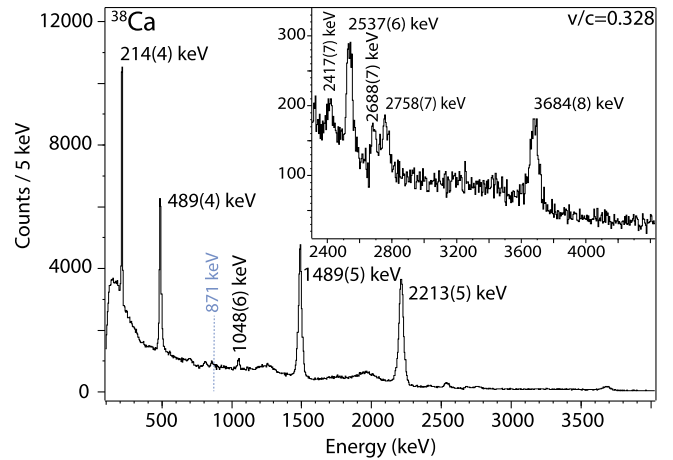


FIG. 2. Doppler-reconstructed adback  $\gamma$ -ray spectrum as detected in coincidence with the scattered  $^{38}\text{Ca}$  nuclei that underwent a large momentum loss. All  $\gamma$ -ray transitions are labeled by their energy. The inset magnifies the high-energy region of the spectrum.

populated states. The reader is referred to the companion paper for details on some other weakly populated states [10].

To construct the level scheme,  $\gamma\gamma$  coincidences are used. Figure 3 shows the coincidence analysis of the low-energy part of the  $^{38}\text{Ca}$  spectrum. From Fig. 3, it is clear that the 1489-keV  $\gamma$  ray feeds the 2213-keV line, the 489-keV transition feeds the level depopulated by the 1489 keV, and the 214-keV transition lies on top of the level depopulated by the 489-keV transition. There is evidence for a weak 1048-keV transition being in coincidence with the 2213- and 1489-keV  $\gamma$  rays.

Figure 3 also shows the partial level scheme with the intensities of the  $\gamma$ -ray transitions indicated by the arrow widths. These relative  $\gamma$ -ray intensities were deduced from the efficiency-corrected peak areas from the spectrum displayed in Fig. 2. Remarkably, the fourth strongest  $\gamma$  ray, at 214 keV, has not been reported previously. The relative intensities and a more complete level scheme, including all  $\gamma$ -ray transitions observed, is provided in Ref. [10].

The 1489-keV transition in coincidence with the  $2_1^+ \rightarrow 0_1^+$  decay is consistent with the previously reported ( $3^-$ ) state at 3702 keV. The 489-keV transition in coincidence with the 3702-keV ( $3^-$ ) state suggests a level at 4191 keV, which is consistent with a previously reported state at 4194 keV. However, the  $J^\pi$  assignment proposed in the literature of ( $5^-$ ) [16] is unlikely as the 489-keV transition in our work is prompt, on the level of a few ps or faster as evident from the good resolution and absence of a low-energy tail, which—if of  $E2$  character—would indicate a  $B(E2; 5^- \rightarrow 3^-)$  strength exceeding the recommended upper limit of 100 W.u. [17]. From the comparison with the mirror nucleus,  $^{38}\text{Ar}$ , which has a 4480-keV  $4^-$  level

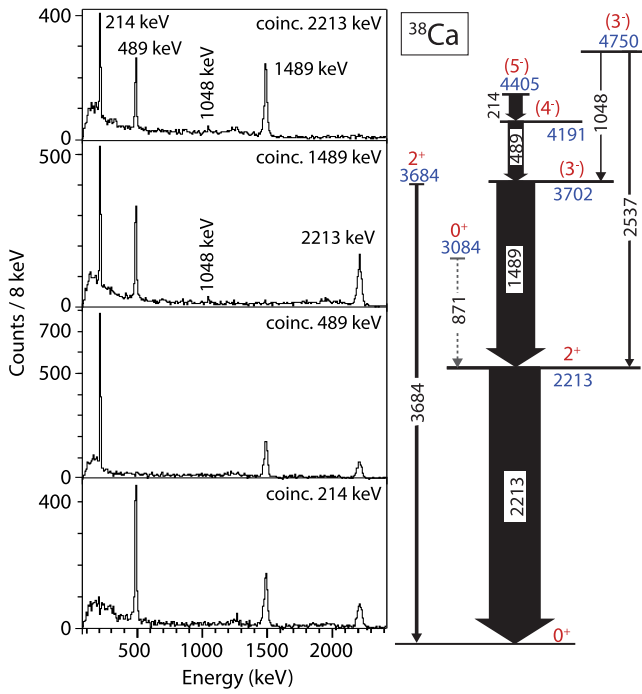


FIG. 3. Left: Doppler-corrected  $\gamma\gamma$  coincidence spectra obtained from cuts on the labeled prominent transitions in the  $\gamma\gamma$  coincidence matrix. Background was subtracted via a cut of equal width at slightly higher energy. Coincidence relationships are evident in the panels. Right: resulting level scheme. The width of the arrows is proportional to the  $\gamma$ -ray intensity of the corresponding transition. The proton separation energy of  $S_p = 4.54727(22)$  MeV [18] places the second  $3^-$  state above the proton separation energy. The  $0_2^+$  state is shown but was not populated in the present Letter.

with a sole transition of 670 keV connecting to the first  $3^-$  state, resembling the situation described here, we propose  $J^\pi = (4^-)$  for the 4191-keV state in  $^{38}\text{Ca}$ . The new 214-keV transition feeding the  $(4^-)$  level establishes a state at 4405 keV, which appears to correspond to the 4586-keV  $5^-$  level in the  $^{38}\text{Ar}$  mirror whose far-dominant decay is a 106-keV transition to the  $4^-$ . Based on mirror symmetry, a  $(5^-)$  assignment is proposed here for the 4405-keV level in  $^{38}\text{Ca}$ . This establishes  $(5^-) \rightarrow (4^-) \rightarrow (3_1^-) \rightarrow 2_1^+$  as the most intense cascade seen following the  $^{38}\text{Ca}$  inelastic scattering populated at large momentum loss.

The next strongest populated level is the  $2_2^+$  state at 3684 keV for which only the transition to the ground state is observed here. A  $0^+$  state at 4748(5) keV is claimed in  $^{38}\text{Ca}$  from the  $(^3\text{He}, n)$  transfer reaction, however, with the suspicion of a doublet [16]. Because of the transition to the  $(3^-)$  state, a  $0^+$  assignment is excluded, and the level established here is tentatively assigned  $(3_2^-)$ , consistent with the 4877-keV  $3_2^-$  level in the  $^{38}\text{Ar}$  mirror, which also decays predominantly to the  $2_1^+$  and  $3_1^-$  states [16].

It is interesting to explore which low-lying levels have not been observed in the present experiment. This is, most

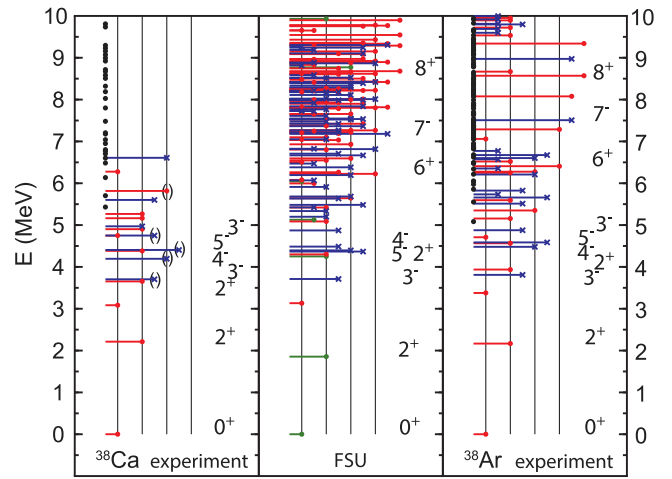


FIG. 4. Comparison of the energies of the low-lying states of  $^{38}\text{Ca}$ , with the states observed here labeled, with shell-model calculations using the FSU  $spsdfp$  interaction, and states in  $^{38}\text{Ar}$  [16]. In these plots, the length of the levels indicates the  $J$  value and the color positive parity  $\Delta = 2$  (red), negative parity  $\Delta = 1$  (blue), and  $sd$ -shell origin  $\Delta = 0$  (green).

prominently, the  $0_2^+$  state reported at 3084 keV which would decay to the first  $2^+$  state with a 871-keV transition [16]. There is no evidence for an appreciable presence of that transition in Figs. 2 and 3 (the 871-keV transition would be 13 keV above the background feature originating from neutron-induced background as indicated in Fig. 2).

In the following, we discuss the configurations of the states observed. Many properties of  $^{40}\text{Ca}$  and the surrounding nuclei can be interpreted relative to a doubly closed shell structure for the ground state of  $^{40}\text{Ca}$  with the  $sd$  shell filled and the  $pf$  shell empty. The first excited state of  $^{40}\text{Ca}$  has  $J^\pi = 0^+$  and is qualitatively associated with a four-particle four-hole ( $4p$ - $4h$ ) state relative to the  $^{40}\text{Ca}$  closed-shell ground state [19]. We will use  $\Delta$ , the number of nucleons moved from  $sd$  to  $fp$  orbitals, to characterize the structure of the states. In this notation, the  $4p$ - $4h$  states in  $^{40}\text{Ca}$  have  $\Delta = 4$ . (To remove spurious states, the  $\Delta$  basis includes all components associated with the  $\Delta\hbar\omega$  basis constructed in the  $0s$ - $0p$ - $0d$ - $1s$ - $0f$ - $1p$  model space).

In Ref. [20], a Hamiltonian was developed for these pure  $\Delta$  configurations. This Hamiltonian served as the starting point for the new Florida State University (FSU) Hamiltonian for pure  $\Delta$  states [21,22]. The  $A = 38$  FSU results are compared to the experiment in Fig. 4, the overall agreement with the experiment being good. The calculated configurations can be divided into those with  $\Delta = 0$  with positive parity (green), those with  $\Delta = 1$  with negative parity (blue), and those with  $\Delta = 2$  with positive parity (red).

In the present  $^{38}\text{Ca}$  level scheme, the strongest  $\gamma$  rays come from the  $2_1^+$  state, which is predicted to be of  $sd$ -shell origin, and from states with  $\Delta = 1$ , including the highest

$J^\pi = 5^-$  level possible for this  $\Delta$ . The  $\gamma$ -ray decay of the  $2_2^+$  state is also observed. In the  $^{36}\text{Ar}(^3\text{He}, n)$  reaction in Ref. [23], this state is found to have a strong  $(f_{7/2})^2$  form factor which would come from  $\Delta = 2$  configurations in the FSU spectrum. However, the  $0_2^+$  state, which also has  $\Delta = 2$ , was not populated.

In the following, we propose a view that puts the populated states within the context of the observed high-momentum-loss reaction events. From the approximately 200 MeV of energy loss in the reaction, and given that the detected  $^{38}\text{Ca}$  are largely within laboratory scattering angles of  $3^\circ$ – $4^\circ$ , about 150 MeV must be dissipated in the  $^9\text{Be}$  nuclei, with a total binding of 58 MeV. Thus, there must be disintegration of the target nucleus into a number of energetic fragments. The emerging picture is then one of multiple nucleons interacting in a single collision with the formation of complex multiparticle-multihole configurations, in contrast to the situation in far-less-dissipative, surface-grazing collisions. We exclude scenarios where a  $^{38}\text{Ca}$  projectile undergoes multiple collisions within the target as an explanation for the observed cross sections. High-momentum-loss events creating  $mp - nh$  excitations in such a scenario would require a sequence of knockout and/or pickup processes, and such pickup mechanism cross sections are small—with a typical upper limit of 2 mb at these beam energies [24].

Connecting with the shell-model picture, excitations within the FSU model space are described by many-body transition densities. In the simplest scenario, excitation of the  $\Delta = 1$  negative-parity states involve the  $\Delta = 0$  to  $\Delta = 1$  one-body transition densities (OBTDs). The OBTDs to those states observed are all large. The  $\Delta = 2$ ,  $2_2^+$  state involves the  $\Delta = 0$  to  $\Delta = 2$  two-body transition density (TBTD). The TBTD connecting the  $\Delta = 0$  and  $\Delta = 2$   $0^+$  wave functions are the same ones that enter the Hamiltonian matrix for mixing these two states. We expect that the microscopic, two-nucleon excitation mechanism should involve an operator similar to that of the two-body mixing Hamiltonian (e.g., dominated by pairing). This would explain why excitation of the  $0_2^+$  is not observed; the mixed  $0_1^+$  and  $0_2^+$  eigenfunctions are orthogonal with respect to the two-nucleon excitation operator. We note that in  $^{40}\text{Ca}(p, t)$  [25], the  $0_2^+$  state is only very weakly populated compared to the  $2_2^+$  state (see Fig. 1 in Ref. [25]).

The events at momentum losses of 600–700 MeV/c studied here are also reminiscent of observations in the work of Podolyak *et al.* [26]. There, in the two-neutron knockout from  $^{56}\text{Fe}$  to  $^{54}\text{Fe}$  at 500 MeV/nucleon, the population of a  $10^+$  isomer of complex structure was observed in the low-momentum tail of the parallel momentum distribution at about the same absolute momentum loss. The authors attributed this population to the excitation of the  $\Delta(1232)$  resonance at their relativistic beam energies. This mechanism is not available to our

intermediate-energy beams of tens of MeV/nucleon. One may speculate that the population of the complex-structure state in the two-neutron knockout from  $^{56}\text{Fe}$  is rather due to a simultaneous multinucleon rearrangement as hypothesized here, without evoking quark degrees of freedom and consistent with the reduction of multistep processes at their relativistic energies. For example, population of the  $10^+$  state could be due to the  $\Delta J = 6$  excitation of a  $(f_{7/2})^2 6^+$  configuration in  $^{56}\text{Fe}$  combined with the removal of two neutrons from the  $1p_{3/2}$  and  $0f_{7/2}$  orbitals having  $\Delta J \geq 4$ .

In Ref. [10], from the high-spin spectroscopy of states up to  $J = 15/2$  in  $^{39}\text{Ca}$ , we argue that such a simultaneous multinucleon rearrangement is also at play in intermediate-energy nucleon transfer reactions, such as  $^9\text{Be}(^{38}\text{Ca}^*, ^{39}\text{Ca} + \gamma)X$ . Once again, these excitations are seen in events in the tail of the longitudinal momentum distribution at a momentum loss of 600–700 MeV/c.

In the present Letter, the specific reaction dynamics at play in the observed large momentum loss collisions are unclear and remain a challenge for future, more complete and exclusive measurements. Specifically, it would be critical to detect the dissociation of the  $^9\text{Be}$  target nuclei in the large-momentum-loss events and clarify the kinematics of the residues.

While there is much to be discovered about this type of reaction, it is evident that this presents a new opportunity in the fast-beam regime which uniquely complements classic low-energy reactions, such as multistep Coulomb excitation and multinucleon transfer. Fast beams allow for the use thick targets and capitalize on an increase in  $\gamma$ -ray yield by a factor of about 4300 for the specific example of a 188-mg/cm<sup>2</sup>  $^9\text{Be}$  target used here vs a 1-mg/cm<sup>2</sup> Pb target often employed for multistep Coulomb excitation, for example. Also, strong forward focusing enhances the collection efficiency as compared to low-energy reactions that fill a larger phase space.

Multistep Coulomb excitation studies with low-energy rare-isotope beams have been performed at beam intensities similar to those used here, but have been limited to a complementary level scheme selectively comprising cascades connected by strong  $E2$  transitions, with at most the first  $3^-$  state [7,27]. We illustrate this with the example of the state-of-the-art low-energy Coulomb excitation of the neighboring Ca isotope  $^{42}\text{Ca}$  on Pb [28]. The measurement was performed at 1 pA stable-beam intensity for five days (resulting in more than 110 000 times the number of Ca projectiles on target as in the present measurement). Excited states up to the  $4_{1,2}^+$  states were reported with no evidence for any of the negative-parity cross-shell excitations observed here.

Multinucleon transfer, largely limited to stable beams at pA beam intensities, is known to populate complex-structure states, however, without efficiently reaching  $^{38}\text{Ca}$  despite  $^{40}\text{Ca}$  being an often-used beam (see Ref. [29] and references within). When low-energy neutron-rich

beams become available at near-stable-beam intensities, multinucleon transfer may become an alternative to access such states in selected neutron-rich nuclei [30]. While it is interesting to also extend our approach to collective nuclei, it already promises to be a unique method to probe cross-shell excitations near magic numbers, elucidating shell evolution in rare isotopes and exploring the necessary model spaces for a region's description on the quest for a predictive model of nuclei.

In conclusion, the in-beam  $\gamma$ -ray spectroscopy is reported of higher-spin, complex-structure negative-parity states in  $^{38}\text{Ca}$  populated in highly dissipative processes induced by a fast  $^{38}\text{Ca}$  projectile beam reacting with a  $^9\text{Be}$  target. This Letter constitutes the first high-resolution  $\gamma$ -ray spectroscopy of  $^{38}\text{Ca}$  with a modern HPGe  $\gamma$ -ray tracking array. The final states observed in the inelastic scattering  $^9\text{Be}(^{38}\text{Ca}, ^{38}\text{Ca} + \gamma)X$  at large momentum loss are characterized through their particle-hole character relative to the  $^{40}\text{Ca}$  closed-shell ground state. Excellent agreement is obtained with shell-model calculations using the FSU cross-shell effective interaction. Based on the strongly populated negative-parity states and the nonobservation of the first excited  $0_2^+$  state, we propose a consistent picture in which these multiparticle-multihole states are formed by simultaneous rearrangement of multiple nucleons in a single, highly dissipative collision. These reaction processes seen here in the extreme low-momentum tail of  $^{38}\text{Ca} + ^9\text{Be}$  inelastic scattering identify a new pathway to gain access to excited states not usually observed in fast-beam-induced reactions and likely out of reach for low-energy reactions.

This work was supported by the U.S. National Science Foundation under Grants No. PHY-1565546 and No. PHY-2110365, by the DOE National Nuclear Security Administration through the Nuclear Science and Security Consortium, under Award No. DE-NA0003180, and by the U.S. Department of Energy, Office of Science, Office of Nuclear Physics, under Grants No. DE-SC0020451 (MSU) and No. DE-FG02-87ER-40316 (WashU) and under Contract No. DE-AC02-06CH11357 (ANL). GRETINA was funded by the DOE, Office of Science. Operation of the array at N. S. C. L. was supported by the DOE under Grant No. DE-SC0019034. J. A. T. acknowledges support from the Science and Technology Facilities Council (U.K.) Grant No. ST/V001108/1.

\*Present address: Lawrence Livermore National Laboratory, Livermore, California 94550, USA.

†Present address: TRIUMF, 4004 Wesbrook Mall, Vancouver, BC V6T 2A3, Canada.

[1] A. Gade, *Eur. Phys. J. A* **51**, 118 (2015).

- [2] A. Obertelli, *Eur. Phys. J. Plus* **131**, 319 (2016).
- [3] B. Rubio and W. Gelletly, in *The Euroschool Lectures on Physics with Exotic Beams*, edited by J. Al-Khalili and E. Roeckl (Springer, Berlin, 2009), Vol. III; *Lect. Notes Phys.* **764**, 99 (2009).
- [4] T. Glasmacher, *Annu. Rev. Nucl. Part. Sci.* **48**, 1 (1998).
- [5] P. G. Hansen and J. A. Tostevin, *Annu. Rev. Nucl. Part. Sci.* **53**, 219 (2003).
- [6] A. Gade and T. Glasmacher, *Prog. Part. Nucl. Phys.* **60**, 161 (2008).
- [7] A. Gorgen and W. Korten, *J. Phys. G* **43**, 024002 (2016).
- [8] K. Wimmer, *J. Phys. G* **45**, 033002 (2018).
- [9] A. Gade, D. Weisshaar, B. A. Brown, J. A. Tostevin, D. Bazin, K. Brown, R. J. Charity, P. J. Farris, A. M. Hill, J. Li, B. Longfellow, W. Reviol, and D. Rhodes, *Phys. Lett. B* **808**, 135637 (2020).
- [10] A. Gade *et al.*, companion paper, *Phys. Rev. C* **106**, 064303 (2022).
- [11] A. Gade and B. M. Sherrill, *Phys. Scr.* **91**, 053003 (2016).
- [12] D. Bazin, J. A. Caggiano, B. M. Sherrill, J. Yurkon, and A. Zeller, *Nucl. Instrum. Methods Phys. Res., Sect. B* **204**, 629 (2003).
- [13] J. Yurkon, D. Bazin, W. Benenson, D. J. Morrissey, B. M. Sherrill, D. Swan, and R. Swanson, *Nucl. Instrum. Methods Phys. Res., Sect. A* **422**, 291 (1999).
- [14] S. Paschalis *et al.*, *Nucl. Instrum. Methods Phys. Res., Sect. A* **709**, 44 (2013).
- [15] D. Weisshaar *et al.*, *Nucl. Instrum. Methods Phys. Res., Sect. A* **847**, 187 (2017).
- [16] J. Chen, *Nucl. Data Sheets* **152**, 1 (2018).
- [17] P. M. Endt, *At. Data Nucl. Data Tables* **55**, 171 (1993).
- [18] M. Wang, W. J. Huang, F. G. Kondev, G. Audi, and S. Naimi, *Chin. Phys. C* **45**, 030003 (2021).
- [19] W. J. Gerace and A. M. Green, *Nucl. Phys.* **A93**, 110 (1967); **A123**, 241 (1969).
- [20] E. K. Warburton, J. A. Becker, and B. A. Brown, *Phys. Rev. C* **41**, 1147 (1990).
- [21] R. S. Lubna, K. Kravvaris, S. L. Tabor, Vandana Tripathi, A. Volya, E. Rubino, J. M. Allmond, B. Abromeit, L. T. Baby, and T. C. Hensley, *Phys. Rev. C* **100**, 034308 (2019).
- [22] R. S. Lubna, K. Kravvaris, S. L. Tabor, Vandana Tripathi, E. Rubino, and A. Volya, *Phys. Rev. Res.* **2**, 043342 (2020).
- [23] W. P. Alford, P. Craig, D. A. Lind, R. S. Raymond, J. Ullman, C. D. Zafiratos, and B. H. Wildenthal, *Nucl. Phys.* **A457**, 317 (1986).
- [24] A. Gade, J. A. Tostevin, V. Bader, T. Baugher, D. Bazin, J. S. Berryman, B. A. Brown, D. J. Hartley, E. Lunderberg, F. Recchia, S. R. Stroberg, Y. Utsuno, D. Weisshaar, and K. Wimmer, *Phys. Rev. C* **93**, 031601(R) (2016).
- [25] S. Kubono, S. Kato, M. Yasue, H. Ohnuma, M. Sasao, K. Tsukamoto, and R. Kuramasu, *Nucl. Phys.* **A276**, 201 (1977).
- [26] Zs. Podolyak *et al.*, *Phys. Rev. Lett.* **117**, 222302 (2016).
- [27] M. Rocchini and M. Zielinska, *Physics* **3**, 1237 (2021).

- [28] K. Hadynska-Klek, P.J. Napiorkowski, M. Zielinska, J. Srebrny, A. Maj *et al.*, *Phys. Rev. C* **97**, 024326 (2018).
- [29] L. Corradi, S. Szilner, G. Pollarolo, D. Montanari, E. Fioretto, A.M. Stefanini, J.J. Valiente-Dobon, E. Farnea, C. Michelagnoli, G. Montagnoli, F. Scarlassara, C. A. Ur, T. Mijatovic, D. Jelavic Malenica, and N. Soic F. Haas, *Nucl. Instrum. Methods Phys. Res., Sect. B* **317**, 743 (2013).
- [30] P. Colovic, S. Szilner, A. Illana, J.J. Valiente-Dobon, L. Corradi *et al.*, *Phys. Rev. C* **102**, 054609 (2020).